GeoJournal (2023) 88:2449–2470
https://doi.org/10.1007/s10708-022-10757-7

Dengue risk zone mapping of Thiruvananthapuram district, India: a comparison of the AHP and F-AHP methods

G. Harsha · T. S. Anish · A. Rajaneesh · Megha K. Prasad · Ronu Mathew · Pratheesh C. Mammen · R. S. Ajin · Sekhar L. Kuriakose

Accepted: 6 September 2022 / Published online: 16 September 2022

Abstract Dengue fever, which is spread by *Aedes* mosquitoes, has claimed many lives in Kerala, with the Thiruvananthapuram district bearing the brunt of the toll. This study aims to demarcate the dengue risk zones in Thiruvananthapuram district using the analytical hierarchy process (AHP) and the fuzzy-AHP (F-AHP) methods. For the risk modelling, geo-environmental factors (normalized difference vegetation index, land surface temperature, topographic wetness index, land use/land cover types, elevation, normalized difference built-up index) and demographic factors (household density, population density) have been utilized. The ArcGIS 10.8 and ERDAS Imagine 8.4 software tools have been used to derive the risk zone maps. The area of the risk maps is classified into five zones. The dengue risk zone maps were validated using dengue case data collected from the Integrated Disease Surveillance Programme portal. From the receiver operating characteristic (ROC) curve analysis and the area under the ROC curve (AUC) values, it is proved that the F-AHP method (AUC value of 0.971) has comparatively more prediction capability than the AHP method (AUC value of 0.954) in demarcating the dengue risk zones. Also, based on the comparison of the risk zone map with actual case data, it was confirmed that around 82.87% of the dengue cases occurred in the very high and high-risk zones, thus proving the efficacy of the model. According to the dengue risk map prepared using the F-AHP model, 9.09% of the area of Thiruvananthapuram district is categorized as very high risk. The prepared dengue risk maps will be helpful for decision-makers, staff with the health, and disaster management departments in adopting effective measures to prevent the

G. Harsha
School of Fishery Environment, Kerala University of Fisheries and Ocean Studies, Kochi, Kerala, India

T. S. Anish
Department of Community Medicine, Government Medical College, Thiruvananthapuram, Kerala, India

A. Rajaneesh
Department of Geology, University of Kerala, Thiruvananthapuram, India

M. K. Prasad · R. Mathew
Department of Remote Sensing, Bharathidasan University, Tiruchirappalli, Tamil Nadu, India

R. Mathew · P. C. Mammen · R. S. Ajin (✉) · S. L. Kuriakose
Kerala State Emergency Operations Centre, Kerala State Disaster Management Authority, Thiruvananthapuram, India
e-mail: ajinares@gmail.com; ajinares@ieee.org

R. S. Ajin
Resilience Development Initiative (RDI), Bandung, Indonesia

S. L. Kuriakose
Faculty for Geo-Information Science and Earth Observation (ITC), Centre for Disaster Resilience (CDR), University of Twente, Enschede, Netherlands

risks of dengue spread and thereby minimize loss of life.

Keywords *Aedes* mosquito · Analytical hierarchy process · Dengue outbreak · F-AHP · ROC

Introduction

Dengue fever is a mosquito-borne disease that affects about half of the global population (Messina et al., 2019). It is most common in tropical and sub-tropical countries' urban and semi-urban areas (Balaji & Saravanabavan, 2020). Dengue fever has surged 30 times in the last decade, with an estimated 390 million infections each year (Pilot et al., 2020). Dengue fever is caused by four kinds of dengue virus that are serologically distinct (DENV-1, DENV-2, DENV-3, and DENV-4) and it is transferred to people by *Aedes* mosquitoes, such as *Aedes aegypti* (L.) and *Aedes albopictus* (Skuse) (Kumar et al., 2013). The fifth dengue virus serotype, DENV-5, was found by Mustafa et al., (2015). Infected female *Aedes aegypti* and *Aedes albopictus* mosquitoes may transmit the virus to the next generation by transovarial transmission (Getachew et al., 2015). Because it favours animals over humans, unlike *Aedes aegypti*, which has a strong preference for humans (L., 1762), it is widely assumed that *Aedes albopictus* serves as a secondary vector of human arboviruses such as dengue virus (DENV) (Hawley, 1988).

Aedes aegypti is of different polytypic forms, namely domestic (a light-coloured indoor type which breeds in water pots kept inside the houses), sylvan (a dark-coloured type which breeds in tree holes usually seen in forests adjacent to villages), and peridomestic (an intermediate type which breeds in disturbed or modified areas such as coconut groves, farms, etc.) (Tabachnick et al., 1979). Dengue fever, dengue haemorrhagic fever, and mild acute febrile illness can all be caused by the dengue virus (Chaturvedi et al., 2000). Patients may experience headaches, high temperatures, joint pain, vomiting, and myalgia during the initial febrile phase (Nakano, 2018). Dengue shock syndrome, which includes plasma leakage, coagulation problems, and enhanced vascular fragility, is one of the most significant clinical symptoms (Bhatt et al., 2021).

The World Health Organization (WHO) estimates that 50–100 million dengue infections occur each year (Bhatt et al., 2013). According to a recent study (Zeng et al., 2021), there were 104.77 million dengue cases worldwide in 2017, compared to 23.28 million cases in 1990. Asia bears the majority of the dengue disease's worldwide burden (https://www.who.int/). South-East Asia and the Western Pacific are the dengue-endemic regions, with developing countries being the most exposed (Lai, 2018). According to WHO (https://www.who.int/), India is one of the 30 nations with the highest dengue endemicity rates in the world. Also, on the list of the top ten nations with the largest number of viral disease deaths, India ranks first (with 436,343 fatalities between 1900 and 2022) (https://public.emdat.be/). The state of Kerala in India is hyperendemic and one of the leading states in dengue death reporting (Karunakaran et al., 2014). The dengue outbreak that occurred in Kerala in the year 2017 reported 21,993 confirmed cases and 165 deaths (Kumar et al., 2019). Although all the 14 districts in Kerala have recorded cases, more than 50% come from Thiruvananthapuram district (Kumar et al., 2019). According to Banerjee (2017), one possible reason was the drought, which caused people to store drinking water in large containers to deal with the water crisis, which resulted in mosquito breeding. In Kerala, the first epidemic occurred in the year 2003, with 3546 confirmed cases and 68 deaths, with the Thiruvananthapuram district being the worst affected (Nujum et al., 2020). In 2006, 65% of the total dengue cases were reported in the Kerala district of Thiruvananthapuram (Samuel et al., 2014). Hence, there is a need to assess the risk in the Thiruvananthapuram district to minimize the spread of dengue and thereby prevent the loss of lives.

This study compared two models (AHP and F-AHP) and factors like normalized difference vegetation index (NDVI), land surface temperature (LST), topographic wetness index (TWI), and normalized difference built-up index (NDBI), which have never been applied in any part of the world. The present study aimed to identify the dengue risk zones in the Thiruvananthapuram district using the AHP and the F-AHP methods and to compare the prediction accuracy of both methods. This study used factors such as NDVI, LST, TWI, LULC, elevation, NDBI, household density, and population density.

Literature review

The study by Bhatt et al., (2013) predicted dengue to be prevalent across the tropics, with local spatial differences in risk being substantially impacted by rainfall, temperature, and the level of urbanization, and estimated 390 million dengue infections per year, of which 96 million appear to be obvious. Fan et al., (2015) observed a significant increase in dengue risk between 22 and 29 °C. The study by Rogers et al., (2014) conducted for Europe found very few parts of rural Europe are now suited for dengue, and several big cities appear to be at some level of risk, perhaps as a result of a combination of climatic conditions (precipitation and temperature) and dense population. According to a study done in Brazil by Lowe et al., (2021), dengue risk is higher in more rural areas than in highly urbanized areas during periods of major flooding, while it is higher in highly urbanized areas than in rural areas during extremely drought conditions. In a study in a Brazilian urban slum, Kikuti et al., (2015) found that the risk of dengue is higher in places where people are poor.

The research conducted by Koyadun et al., (2012) in Thailand found that in the areas that experienced historical dengue outbreaks, houses with window screens, people aged > 45, individuals with middle and higher degrees, households with more than 4 members, and people engaged in clean-up campaigns were likely to experience a higher risk of dengue transmission. Another study conducted in Thailand identified the reason for higher dengue incidence and risk levels in Bangkok as being due to La Niña and El Niño impacts (Langkulsen et al., 2020). Wijayanti et al., (2016) identified employment type and economic status as the most influential factors on dengue risk in Banyumas regency, Central Java (Indonesia). The study conducted in Vietnam (Schmidt et al., 2011) observed a higher dengue risk in rural areas with a lack of piped water supply than in urban areas. Lack of access to tap water was identified as the major reason for dengue risk in Delhi (India) (Telle et al., 2021).

Many researchers (Ali & Ahmad, 2018; Dom et al., 2016; Hassan et al., 2012; Khormi & Kumar, 2012; Latif & Mohamad, 2015; Ong et al., 2018; Panhwer et al., 2017; Pathirana et al., 2009; Saravanabavan et al., 2019; Shafie, 2011; Tariq & Zaidi, 2019; Tsheten et al., 2021; Withanage et al., 2021) identified the dengue risk zones using GIS techniques. Ali and Ahmad, (2018) demarcated the dengue risk zones in the Kolkata Municipal Corporation using the GIS and AHP method. They used factors such as population density, household density, land use and land cover (LULC), elevation, buffer from waterlogged areas, and land surface temperature. Dom et al., (2013) also identified dengue risk zones in Subang Jaya (Malaysia) using GIS techniques, where they found a higher distribution in residential areas due to higher population density and favourable places for dengue breeding. Ong et al., (2018) mapped the dengue risk zones in Singapore using the random forest model with a Kappa coefficient of more than 0.80. They utilized population, entomological, and environmental factors. Withanage et al., (2021) demarcated dengue risk zones in Gampaha district (Sri Lanka) using GIS-based multivariate analysis. They selected factors such as breeding places, roads, total buildings, land use (home gardens, marshlands, urban areas), public places, and elevation, and found high-risk zones in the close proximity to roads. All these studies applied a single method for identifying the risk zones.

Materials and methods

Study area

The climate of Thiruvananthapuram district is typically hot-tropical, and the monsoon season extends from June to October (Nair & Aravind, 2020). The optimal environment for dengue breeding is one with high temperatures and humidity (Lai, 2018), which can make this district more exposed. The river basins in the district include Neyyar, Karamana, and Vamanapuram, and the major rivers are Neyyar, Karamana, Vamanapuram, Mamom, and Ayirur, and the average annual rainfall is 2035 mm (Rani, 2013). 73 panchayats, four municipalities, and a corporation are part of the administrative divisions (Valson & Soman, 2017). According to the 2011 census data, the district had a population of 3,307,284 (https://trivandrum.nic.in/en/; Rani, 2013). The total area of the district is 2192 km^2 (https://trivandrum.nic.in/en/). It has the highest population density in the state, with 1508 people/sq.km., and the second-highest total population, after the Malappuram district (DCHB 2014). 11.3% of the population in this district belongs to the scheduled

caste, an unprivileged group in India, which is above the state average of 9.1% (https://censusindia.gov.in/; https://scdd.kerala.gov.in/). Also, this district stands second (with 38.36%) in the state in terms of deprivation rate, after Palakkad (42.33%) (https://spb.kerala.gov.in). The location of the Thiruvananthapuram district is depicted in Fig. 1.

Data used

The modelling process involves the following steps (Fig. 2):

i. The data for the eight factors were derived from a variety of sources (Table 1). ERDAS Imagine 8.4 (Leica Geosystems AG, Heerbrugg, Switzerland) and ArcGIS 10.8 (ESRI Inc., Redlands, California, United States) software tools were used to create the thematic layers for these factors.
ii. After obtaining the thematic layers, data on dengue cases for the period 2015–2018 was downloaded from the district level line list of daily dengue cases collected from the Directorate of Health Services (DHS)'s Integrated Disease Surveillance Programme (IDSP) portal (https://dhs.kerala.gov.in/idsp-2/).
iii. For the validation, one location (point) was chosen from each local self-government (LSG) having dengue cases.
iv. The natural breaks (Arabameri et al., 2020; Pradeep et al., 2022; Vojteková & Vojtek, 2020) method was used to classify the thematic layers of factors such as NDVI, LST, TWI, elevation, NDBI, household density, and population density.
v. The AHP and F-AHP methods were employed to create the dengue risk zone maps.
vi. The ROC curve method was used to validate the risk maps. For the creation of ROC curves

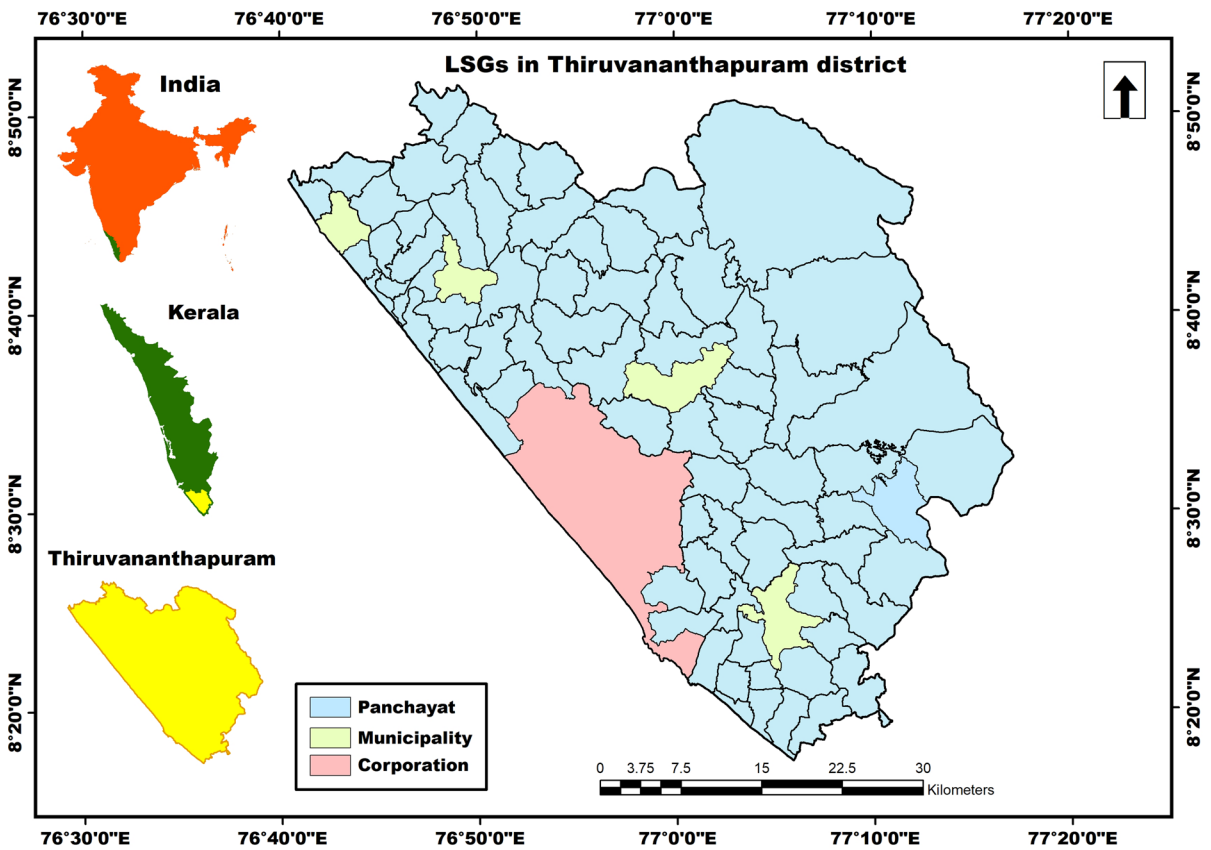

Fig. 1 The study area

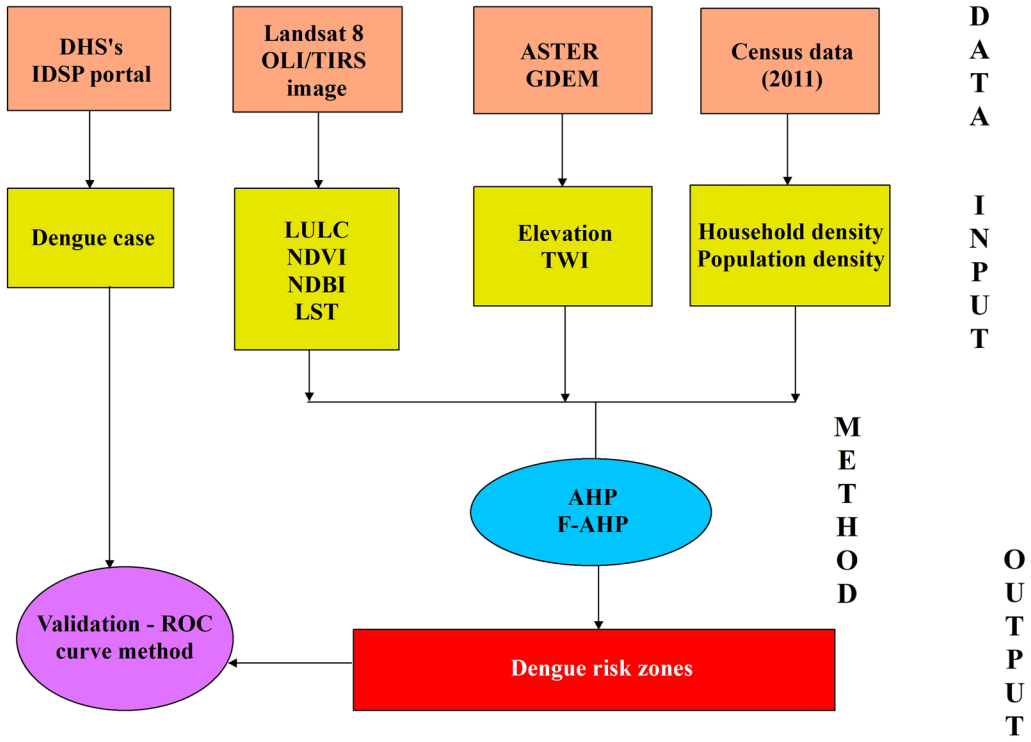

Fig. 2 Flowchart of the dengue risk modelling

Table 1 Data source

Data	Source	Thematic layers derived	Spatial resolution
ASTER GDEM	https://earthexplorer.usgs.gov/	Elevation TWI	30 m
Landsat 8 OLI image	https://earthexplorer.usgs.gov/	LULC NDVI NDBI	30 m
Landsat 8 TIRS image	https://earthexplorer.usgs.gov/	LST	100 m
2011 census data	https://censusindia.gov.in/	Household density Population density	–
Dengue cases data	https://dhs.kerala.gov.in/idsp-2/	–	–

and the estimation of AUC values, the SPSS (IBM Corporation, Armonk, New York, United States) software was utilized.

Derivation of factors selected for the risk modelling

The elevation of the Thiruvananthapuram district was extracted from the GDEM at 30 m (spatial) resolution. The spatial analyst (surface) tool available with the ArcGIS software was used to derive the elevation. The ERDAS Imagine software was used to classify the different land use/land types from the Landsat image acquired on 21st August 2020. The maximum likelihood (ML) classification (Alam et al., 2020; Babitha et al., 2022; Reis, 2008) was adopted in this study. From the 2011 census data (DCHB 2014), the number of households in each panchayat, municipality, and corporation was gathered, and the density was computed using ArcGIS software (as in Ali &

Ahmad, 2018). The population data for each panchayat, municipality, and corporation was collected from the 2011 Census data (DCHB 2014), and the population density layer was created using ArcGIS software (as in Ali & Ahmad, 2018). By dividing the sum of near-infrared (NIR) and red (Red) reflectance by their difference, the NDVI is computed (Gessesse & Melesse, 2019). NDVI was computed using Eq. 1 (Rouse et al., 1974) and ArcGIS raster calculator tool. NDBI was calculated using Eq. 2, and ranges between − 1 and + 1, where positive values represent built-up areas (Zha et al., 2003). The topographic wetness index of the district was computed from the GDEM using ArcGIS raster calculator tool. TWI was computed using Eq. 3 (Beven & Kirkby, 1979).

$$NDVI = \frac{(NIR - Red)}{(NIR + Red)} \tag{1}$$

$$NDBI = \frac{(SWIR1 - NIR)}{(SWIR1 + NIR)} \tag{2}$$

where Red, NIR and SWIR denote spectral reflectance measurements in the red, near-infrared, and short-wave infrared bands, respectively (Drisya et al., 2018; Zha et al., 2003).

$$\mathrm{TWI} = ln(\alpha / tan\beta) \tag{3}$$

where α is the specific catchment area [α = A/L, catchment.

area (A) divided by contour length (L)] and β is the slope.

Land surface temperature The steps involved with the extraction of LST are mentioned below (as in Dang et al., 2020, and Kumar et al., 2021a):

Conversion of the digital number (DN) to spectral radiance (Lλ)

Spectral radiance (.$L\lambda$.) was computed using Eq. 4 (Landsat 8 Data Users Handbook, 2019).

$$L\lambda = gainxQCAL + \text{offset} \tag{4}$$

where, gain = radiance slope/DN transformation function; DN = digital number; and offset = radiance intercept/ DN transformation function (Ghosh et al., 2020).

It can also be expressed as (Eq. 5):

$$L\lambda = LMIN\lambda + \left[\frac{(LMAX\lambda - LMIN\lambda)}{(QCALMAX - QCALMIN)} xQCAL\right] \tag{5}$$

where, QCAL = DN of pixels; QCALMAX = 255; QCALMIN = 0; $LMIN\lambda$ = spectral radiance for thermal band at DN = 0, $LMAX\lambda$ = spectral radiance for thermal band at DN = 255 (Ghosh et al., 2020).

Equation 5 will be more simplified when the corresponding values were replaced in Eq. 4 (Eq. 6)

$$L\lambda = (0.037059 \times DN) + 3.2 \tag{6}$$

Conversion of spectral radiance to At-satellite brightness temperatures

Based on the type of land cover, emissivity (e) for radiant temperatures has been rectified. Vegetation areas were given a score of 0.95, while non-vegetation areas were given a score of 0.92. (Nichol, 1994). As mentioned in Artis and Carnahan (1982), the emissivity corrected LST was identified (Eq. 7).

$$T_B = \frac{K_2}{ln\left(\frac{k_1}{L_\lambda} + 1\right)} \tag{7}$$

where, L_λ is Spectral Radiance in $W.m^{-2}.sr^{-1}.\mu m^{-1}$, and K_1 and K_2 are two constants of two pre-launch calibrations (Ghosh et al., 2020).

LST estimation

The spectral emissivity (ϵ) needs correction since the black body is denoted by the temperature values obtained from the above analyses. The rectification can be done by rendering the land cover type or by computing the corresponding NDVI emissivity values for the respective pixels (Snyder et al., 1998). The emissivity rectified LST was determined using Eq. 8 (Artis & Carnahan, 1982).

$$LST = T_B \Big/ \left[1 + \left\{\left(\frac{\lambda x T_B}{\rho}\right) xln \in\right\}\right] \tag{8}$$

where LST = LST in Kelvin, T_B = At-sensor brightness temperature, λ = TOA reflectance, Inϵ = Emissivity (Ghosh et al., 2020).

Land surface emissivity was computed using Eq. 9.

$$\text{Land surface emissivity } (\in) = 0.004xp_v + 0.986 \quad (9)$$

where p_v is the vegetation proportion, which was calculated using Eq. 10 (Ghosh et al., 2020).

$$p_v - \left(\frac{NDVI_{j_r} - NDVI_{\min}}{NDVI_{\max} - NDVI_{\min}}\right)^2 \quad (10)$$

Conversion of Kelvin to degree Celsius

The measurement unit of these predicted LSTs was transformed to a Kelvin scale using the calculation 0 °C = 273.15 K to simplify the conceptualizing.

Modelling

This study employed methods such as AHP and F-AHP, which are effective in data-scarce conditions (Kumar et al., 2021b; Ramkar & Yadav, 2021). AHP uses pair comparisons to break down complex issues into specific sub-issues, and the components are then prioritized after the hierarchical structure is built (Gompf et al., 2021). F-AHP is similar to AHP, but instead of using numbers, it uses triangular fuzzy numbers. Also, F-AHP can address the inadequacy of AHP to deal with imprecision and subjectivity in assessments (Carnero, 2017).

AHP modelling

AHP, developed by Thomas Saaty (Saaty, 1980), is a method for multi-criteria decision making. This method works to deconstruct complex problems into a hierarchy and identify the solution most suited to the objective (Qazi & Abushammala, 2020). The generation of the matrix for pair-wise comparisons, calculation of the eigen vector, weighting coefficient (Table 2), and consistency ratio (Table 3) are the essential procedures (Akshaya et al., 2021; Senan et al., 2022).where Elev. is the elevation, HD is the household density, and PD is the population density.

Table 2 Pairwise comparison matrix

	NDVI	LST	TWI	LULC	Elev	NDBI	HD	PD	Vp	Cp
NDVI	1	2	3	4	5	6	7	8	3.764	0.328
LST	1/2	1	2	3	4	5	6	7	2.662	0.232
TWI	1/3	1/2	1	2	3	4	5	6	1.819	0.159
LULC	1/4	1/3	1/2	1	2	3	4	5	1.223	0.107
Elev	1/5	1/4	1/3	1/2	1	2	3	4	0.818	0.071
NDBI	1/6	1/5	1/4	1/3	1/2	1	2	3	0.550	0.048
HD	1/7	1/6	1/5	1/4	1/3	1/2	1	2	0.376	0.033
PD	1/8	1/7	1/6	1/5	1/4	1/3	1/2	1	0.266	0.023
∑	2.72	4.59	7.45	11.28	16.08	21.83	28.50	36.00	11.48	1.00

Table 3 Normalized matrix

	NDVI	LST	TWI	LULC	Elev	NDBI	HD	PD	∑ rank	[C]	[D] = [A]*[C]	[E] = [D]/[C]	λ max	CI	CR
NDVI	0.37	0.44	0.40	0.35	0.31	0.27	0.25	0.22	2.61	0.332	2.739	8.252	8.310	0.044	0.031 (3.14%)
LST	0.18	0.22	0.27	0.27	0.25	0.23	0.21	0.19	1.87	0.238	1.905	8.011			
TWI	0.12	0.11	0.13	0.18	0.19	0.18	0.18	0.17	1.24	0.157	1.300	8.262			
LULC	0.09	0.07	0.07	0.09	0.12	0.14	0.14	0.14	0.78	0.099	0.881	8.936			
Elev	0.07	0.05	0.04	0.04	0.06	0.09	0.11	0.11	0.52	0.066	0.595	8.976			
NDBI	0.06	0.04	0.03	0.03	0.03	0.05	0.07	0.08	0.38	0.048	0.401	8.304			
HD	0.05	0.04	0.03	0.02	0.02	0.02	0.04	0.06	0.27	0.035	0.274	7.920			
PD	0.05	0.03	0.02	0.02	0.02	0.02	0.02	0.03	0.20	0.025	0.197	7.820			
∑	1.00	1.00	1.00	1.00	1.00	1.00	1.00	1.00	7.88	1.000		66.481			

Using Eqs. 11 and 12, the eigen vector (*V*p), and the weighting coefficient (*C*p) were determined (Akshaya et al., 2021; Amrutha et al., 2022; Nikhil et al., 2021; Thomas et al., 2021).

$$\mathrm{Vp} = \sqrt[k]{W1x \ldots Wk} \tag{11}$$

where k = number of factors, and W = ratings.

$$\mathrm{Cp} = \frac{Vp}{Vp1 + \ldots Vpk} \tag{12}$$

The normalized matrix, priority vector [C], overall priority [D], and rational priority [E] were calculated as in Danumah et al., (2016).

Using Eqs. 13, 14, and 15, the eigen value (λmax), consistency index (CI), and consistency ratio (CR) were determined (Akshaya et al., 2021; Amrutha et al., 2022; Nikhil et al., 2021; Thomas et al., 2021).

$$\lambda\mathrm{max} = \frac{[E]}{k} \tag{13}$$

$$\mathrm{CI} = (\lambda max - k)/(k-1) \tag{14}$$

$$\mathrm{CR} = \frac{CI}{RI} \tag{15}$$

where RI = random index (Saaty, 1980).

Saaty (1980) accepts a consistency ratio (CR) of less than 0.1. If the CR is higher than 0.1, repeat the analysis until the CR is acceptable. An acceptable CR (0.031) is obtained in this model. Hence, the outcomes are reliable.

The weights obtained using the AHP modelling are depicted in Eq. 16.

$$\begin{aligned}\mathrm{DRZ} =& (0.328 \times NDVI) + (0.232 \times LST) + (0.159 \times TWI) \\ &+ (0.107 \times LULC) + (0.071 \times Elev.) + (0.048 \times NDBI) \\ &+ (0.033 \times HD) + (0.023 \times PD)\end{aligned} \tag{16}$$

F-AHP modelling

To weight the factors in F-AHP model, an ensemble of AHP and fuzzy logic methods was used (Eskandari & Miesel, 2017). By allowing decision-makers to assess their preferences within an acceptable interval, the Fuzzy-AHP model overcomes the constraints of the AHP model (Afolayan et al., 2020). Buckley (1985) proposed a method for comparing fuzzy ratios defined as triangle membership functions, which was used in this research. Pair-wise comparison matrix creation (see Table 4), geometric mean calculation (see Table 5), computation of relative fuzzy weights (see Table 6) and calculation of averaged

Table 5 Geometric means of fuzzy comparison values

	Fuzzy geometric mean value ($\tilde{r}_i$)		
NDVI	2.952	3.764	4.477
LST	1.984	2.662	3.452
TWI	1.334	1.819	2.441
LULC	0.892	1.223	1.668
Elev	0.599	0.818	1.121
NDBI	0.410	0.550	0.750
HD	0.290	0.376	0.504
PD	0.223	0.266	0.339
$\sum \tilde{r}_i$	8.683	11.477	14.752
$(\sum \tilde{r}_i)$ ^-1	0.068	0.087	0.115

Table 4 Pair-wise comparisons of factors

	NDVI	LST	TWI	LULC	Elev	NDBI	HD	PD
NDVI	(1,1,1)	(1,2,3)	(2,3,4)	(3,4,5)	(4,5,6)	(5,6,7)	(6,7,8)	(8,8,8)
LST	(1/3,1/2,1)	(1,1,1)	(1,2,3)	(2,3,4)	(3,4,5)	(4,5,6)	(5,6,7)	(6,7,8)
TWI	(1/4,1/3,1/2)	(1/3,1/2,1)	(1,1,1)	(1,2,3)	(2,3,4)	(3,4,5)	(4,5,6)	(5,6,7)
LULC	(1/5,1/4,1/3)	(1/4,1/3,1/2)	(1/3,1/2,1)	(1,1,1)	(1,2,3)	(2,3,4)	(3,4,5)	(4,5,6)
Elev	(1/6,1/5,1/4)	(1/5,1/4,1/3)	(1/4,1/3,1/2)	(1/3,1/2,1)	(1,1,1)	(1,2,3)	(2,3,4)	(3,4,5)
NDBI	(1/7,1/6,1/5)	(1/6,1/5,1/4)	(1/5,1/4,1/3)	(1/4,1/3,1/2)	(1/3,1/2,1)	(1,1,1)	(1,2,3)	(2,3,4)
HD	(1/8,1/7,1/6)	(1/7,1/6,1/5)	(1/6,1/5,1/4)	(1/5,1/4,1/3)	(1/4,1/3,1/2)	(1/3,1/2,1)	(1,1,1)	(1,2,3)
PD	(1/9,1/8,1/7)	(1/8,1/7,1/6)	(1/7,1/6,1/5)	(1/6,1/5,1/4)	(1/5,1/4,1/3)	(1/4,1/3,1/2)	(1/3,1/2,1)	(1,1,1)

Table 6 Relative fuzzy weights of each factor

	Fuzzy weight ($\tilde{w}_i$)		
NDVI	0.200	0.328	0.516
LST	0.134	0.232	0.398
TWI	0.090	0.159	0.281
LULC	0.060	0.107	0.192
Elev	0.041	0.071	0.129
NDBI	0.028	0.048	0.086
HD	0.020	0.033	0.058
PD	0.015	0.023	0.039

Table 7 Averaged and normalized relative weights of factor

	Weight (Mi)	Normalized weight (Ni)
NDVI	0.348	0.317
LST	0.255	0.232
TWI	0.177	0.161
LULC	0.120	0.109
Elev	0.080	0.073
NDBI	0.054	0.049
HD	0.037	0.034
PD	0.026	0.024
$\sum$	1.10	1.00

and normalised relative weight are the essential procedures involved (see Table 7) (Akshaya et al., 2021; Senan et al., 2022). The steps in F-AHP modelling are as follows:

Step 1 Comparison of the factors.

When factor 1 (P1) is less important than factor 2 (P2), for example, the fuzzy triangular scale will be (2, 3, 4). The fuzzy triangle scale for the comparison matrix will be (1/4, 1/3, 1/2) (Ayhan, 2013).

The matrix is depicted in Eq. 17.

$$\tilde{A}^k = \begin{bmatrix} \tilde{d}^k_{11} & \tilde{d}^k_{12} & \ldots & \tilde{d}^k_{1n} \\ \tilde{d}^k_{21} & \ldots & \ldots & \tilde{d}^k_{2n} \\ \ldots & \ldots & \ldots & \ldots \\ \tilde{d}^k_{n1} & \tilde{d}^k_{n2} & \ldots & \tilde{d}^k_{mn} \end{bmatrix} \tag{17}$$

where,$\tilde{d}^k_{ij}$ indicates the kth decision maker's preference of ith factor over jth factor, by the way of fuzzy triangular numbers (Ayhan, 2013).

Step 2 $\tilde{d}_{ij}$ is calculated using Eq. 18, after averaging the preferences ($\tilde{d}^k_{ij}$)

$$\tilde{d}_{ij} = \frac{\sum_{k=1}^{K} \tilde{d}^k_{ij}}{K} \tag{18}$$

Step 3 Modification of the matrix using Eq. 19.

$$\tilde{A} = \begin{bmatrix} \tilde{d}_{11} & \cdots & \tilde{d}_{1n} \\ \vdots & \ddots & \vdots \\ \tilde{d}_{n1} & \cdots & \tilde{d}_{nn} \end{bmatrix} \tag{19}$$

Step 4 Determination of the geometric average using Eq. 20 (Buckley, 1985).

$$\tilde{r}_i = \left(\prod_{j=1}^{n} \tilde{d}_{ij} \right)^{1/n}, i = 1, 2, ..., n \tag{20}$$

where $\tilde{r}_i$ = triangular values.

Step 5 The fuzzy weight was determined using the next three sub processes (5a, 5b, and 5c).

Step 5a Determination of vector summation of each $\tilde{r}_i$.

Step 5b The summation vector's (-1) power was determined, then the fuzzy triangular number was replaced to convert it to an increasing order.

Step 5c Calculation of fuzzy weight of factors: To determine the fuzzy weight of factors, each $\tilde{r}_i$ was multiplied with the reverse vector as in Eq. 21.

$$\begin{aligned} \tilde{w}_i &= \tilde{r}_i \otimes (\tilde{r}_1 \oplus \tilde{r}_2 \oplus \ldots \oplus \tilde{r}_n)^{-1} \\ &= (lw_i, mw_i, uw_i) \end{aligned} \tag{21}$$

Step 6 Eq. 22 (Chou & Chang, 2008) was used for the de-fuzzification of the fuzzy weights.

$$M_i = \frac{lw_i, mw_i, uw_i}{3} \tag{22}$$

Step 7 Eq. 23 was used for the standardization of Mi (Table 7).

$$N_i = \frac{M_i}{\sum_{i=1}^{n} M_i} \tag{23}$$

The weights obtained using the F-AHP modelling are depicted in Eq. 24.

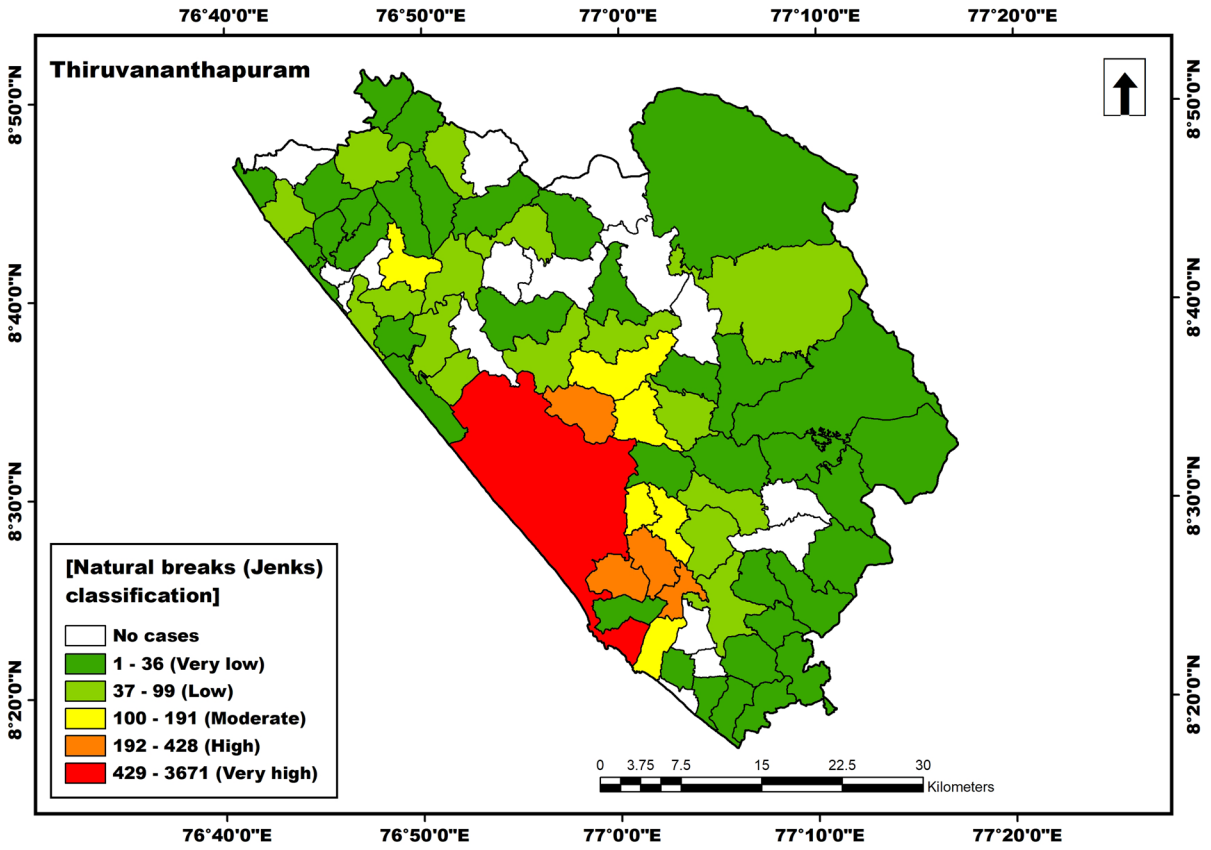

Fig. 3 **a** NDVI, **b** LST, **c** TWI, **d** LULC

$$\begin{aligned} \mathrm{DRZ} =& (0.317 \times NDVI) + (0.232 \times LST) + (0.161 \times TWI) \\ &+ (0.109 \times LULC) + (0.073 \times Elev.) + (0.049 \times NDBI) \\ &+ (0.034 \times HD) + (0.024 \times PD) \end{aligned} \tag{24}$$

Validation using the ROC curve method

The dengue case data (Fig. 3) collected from the DHS's IDSP portal was used to validate the results, which are categorized into five classes (very low, low, moderate, high, and very high). AUC measures the capacity of the test to determine whether there is a specific condition or not (Hoo et al., 2017). The ROC curves were plotted and the AUC values were determined using the SPSS software. The AUC value is excellent for values ranging from 0.9 to 1, good for values ranging from 0.8 to 0.9, fair for values ranging from 0.7 to 0.8, poor for values ranging from 0.6 to 0.7, and failed for values ranging from 0.5 to 0.6 (Battolla et al., 2017). For the validation, one location (point) from each polygon (panchayat, municipality, and corporation) with dengue cases was selected, thus totaling 63 locations (Fig. 4).

Results and discussion

NDVI

The NDVI ranges from −1 to 1 (Choubin et al., 2019), with values closer to zero and negative values indicating features such as barren land, water, snow, and so on (Saravanan et al., 2019), and positive values represent vegetated areas (Viana et al., 2019). The high-density vegetation is usually an unaddressed area, and dengue can breed even in smaller water collection zones, like the case of water accumulated fallen leaves, water filled holes in the tree trunks, etc.

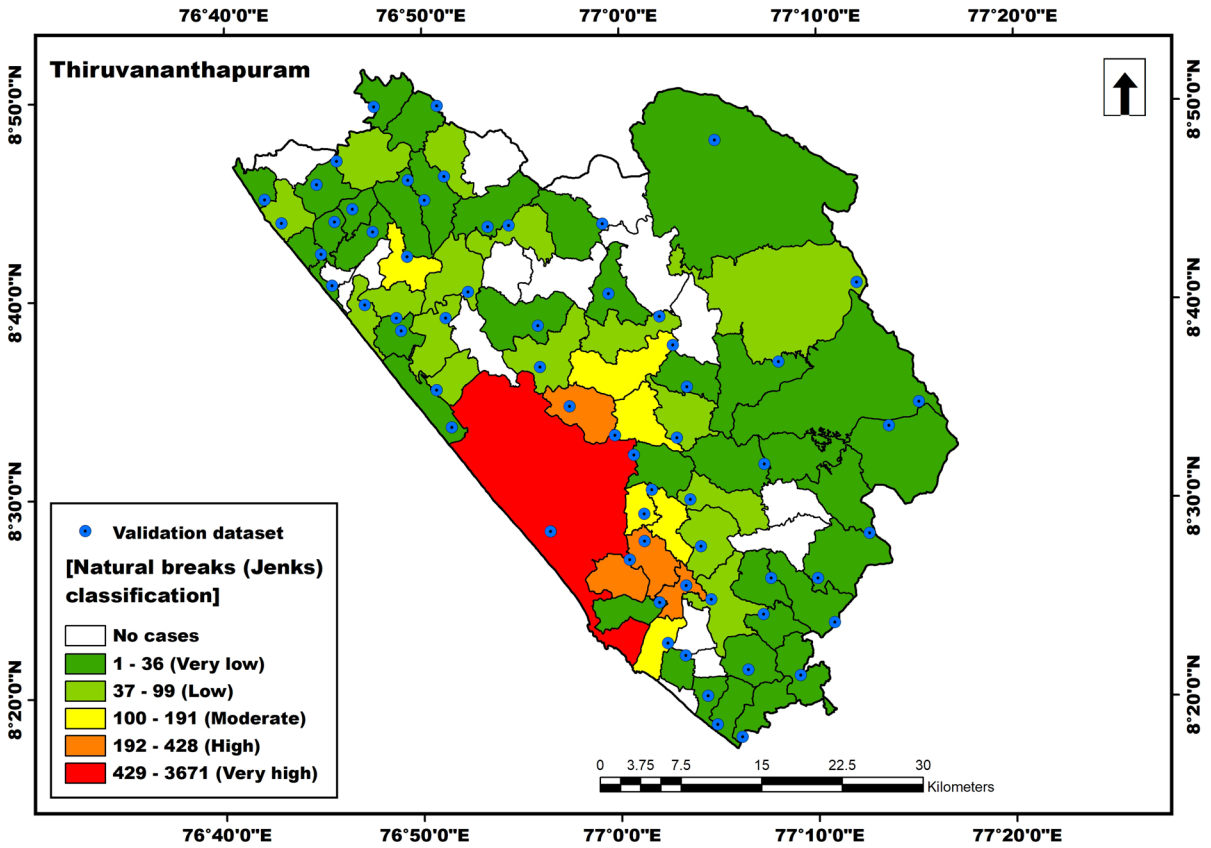

Fig. 4 **a** Elevation, **b** NDBI, **c** Household density, **d** Population density

Aedes aegypti and *Aedes albopictus* had the largest relative abundance in containers of 50–100 mL volume, according to Dissanayake et al., (2021). Hence, the areas with higher NDVI values will have higher dengue spread, as these areas will have a higher number of sylvan *Aedes* mosquitoes. The NDVI of the district ranges between − 0.21 and 1.00 (Fig. 5a).

LST

The *Aedes aegypti* mosquito exhibits shorter developmental times throughout all phases of its life cycle as temperature rises, which promotes faster population growth (Lai, 2018). Shabbir et al., (2020) suggest that the suitable temperature for the breeding of larvae is around 30 °C. The land surface temperature of the Thiruvananthapuram district ranges from 13.37 to 36.59 °C (Fig. 5b) and is categorized into five classes.

TWI

The topographic wetness index can be used as an indicator of a flood potential area (Riadi et al., 2018), as it is an estimate of water accumulation (Cohen et al., 2010). Rasheed et al., (2013) reported an increase in the number of dengue cases following a flood. In their study conducted in Thiruvananthapuram district, Nair and Aravind (2020) found a highly significant correlation between rainfall and dengue cases. This is due to the abundance of outdoor breeding sites created by rains for *Aedes aegypti* (Lai, 2018). The TWI of the Thiruvananthapuram district ranges from 2.02 to 16.94 (Fig. 5c) and is categorized into five classes.

LULC

Land use/land cover types such as built-up areas (commercial sites as well as residential areas) are recognized as likely risk factors in dengue outbreaks

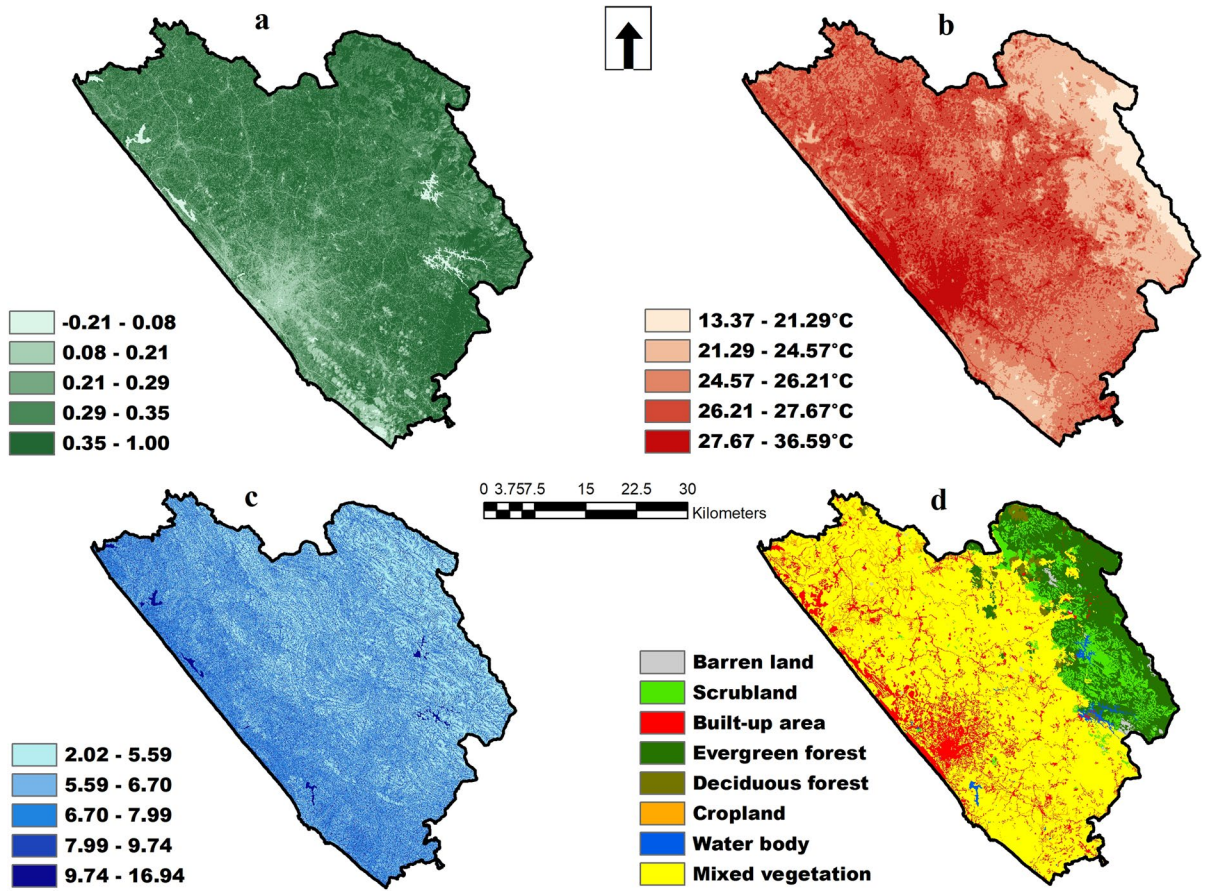

Fig. 5 Dengue cases

because they provide a suitable environment for the vector (Ali & Ahmad, 2018). The croplands were distinguished by sustained water depths of 2.5 cm to 30 cm (Sarfraz et al., 2012), and the study by Sarfraz et al., (2012) indicated that the areas close to the cropland had an increased population of dengue vectors. The LULC types in the district include barren land, scrubland, built-up areas, evergreen forest, deciduous forest, cropland, water bodies, and mixed vegetation (Fig. 5d).

Elevation

A study by Tsheten et al., (2021) found that low-lying areas are more vulnerable and have a higher dengue risk. The elevation of the district ranges up to 1828 m (Fig. 6a), and is divided into five classes: 0–91 m, 91–254 m, 254–545 m, 545–941 m, and 941–1828 m.

NDBI

The NDBI is an index derived from a satellite image that was used to extract built-up areas (Govil et al., 2019). *Aedes aegypti* (L.) will have more vectorial capacity and efficiency than *Aedes albopictus* (Skuse), which means a smaller number of *Aedes aegypti* (L.) can infect more people. As a part of urbanization, there will be a greater availability of smaller water-filled sites, and *Aedes aegypti* (L.) prefers water accumulated in construction sites, water-filled concrete tanks for breeding. Hence, the chance of dengue spreading will be greater in areas with higher NDBI values, as these areas will have a higher risk of peridomestic type mosquitoes. The NDBI of the district ranges between − 1.00 and 0.39 (Fig. 6b).

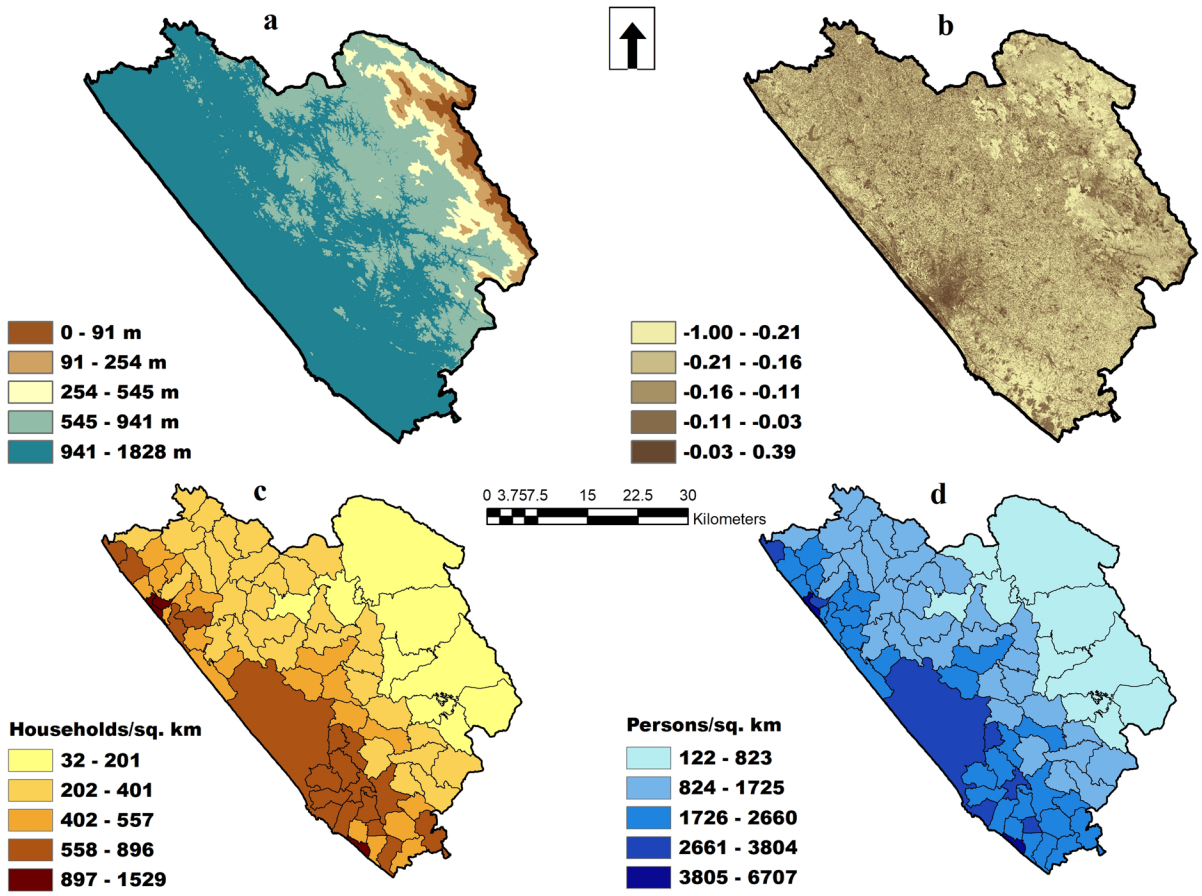

Fig. 6 Validation dataset

Household density

Diseases will spread more easily when household density is higher, as infected *Aedes* mosquitoes usually have a flight range of between 100 and 200 m (Ali & Ahmad, 2018) and can bite people living in crowded areas more easily. Water use, storage, and disposal of water-holding containers all have a substantial impact on *Aedes aegypti* breeding in households (Ngugi et al., 2017). Also, due to the abundance of rain-filled discarded containers, the outdoor environment provides greater breeding possibilities (Ngugi et al., 2017). When households are denser, families may share peri-domestic areas, and this may result in the rapid spread of disease. The areas with higher household density will be at higher risk due to the presence of domestic and peridomestic varieties of *Ae. aegypti*. Honório et al., (2003) discovered that *Aedes aegypti* and *Aedes albopictus* can move at least 800 m in a six-day period in an urban endemic dengue area in the Brazilian state of Rio de Janeiro. The district is categorized into five classes (32–201, 202–401, 402–557, 558–896, and 897–1529) based on the household density, and is depicted in Fig. 6c.

Population density

Higher population density areas may be affected by various issues, including lack of proper sanitation facilities, improper sewage systems, etc. (Ali & Ahmad, 2018). These conditions can create an ideal environment for *Aedes* mosquitoes and result in disease transmission. When the population density is high, the infected mosquitoes will locate numerous individuals to bite during their lifetime. The district is categorized into five classes (122–823, 824–1725,

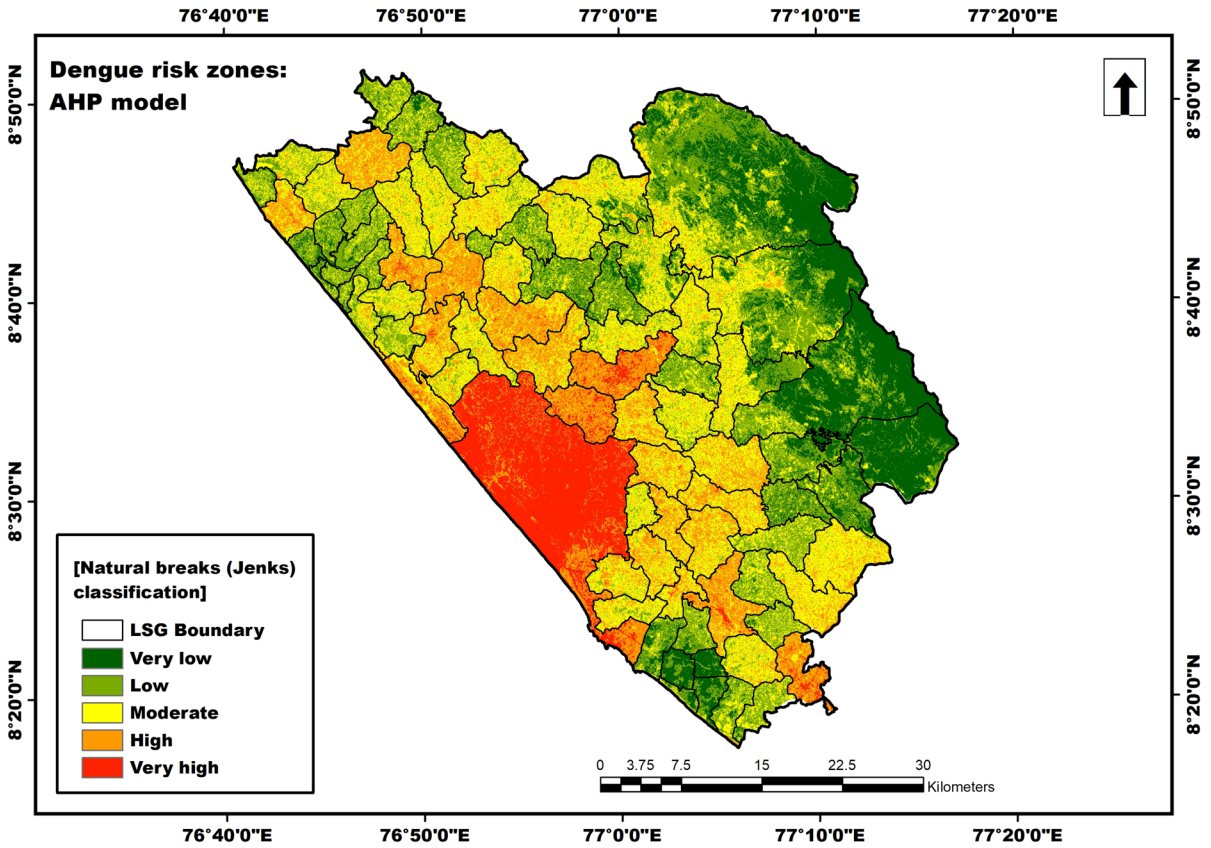

Fig. 7 Dengue risk zones: AHP model

1726–2660, 2661–3804, and 3805–6707) based on population density (Fig. 6d).

Dengue risk zones

The area of Thiruvananthapuram district is grouped into five risk zones ranging from very low to very high. A total of 7661 dengue cases were recorded during the period considered for this study. The prepared dengue risk zone maps are depicted in Figs. 7 and 8. The percentage of risk zones is shown in Table 8. The validation of the results using the ROC curve method proved that both the AHP and the F-AHP models are effective in predicting the risk zone maps with outstanding AUC values of 95.4% (0.954) and 97.1% (0.971), respectively. The study proved that the F-AHP method is more efficient in dengue risk modelling. The ROC curves are depicted in Fig. 9.

As per the risk zone map created applying F-AHP weights, Thiruvananthapuram Corporation is categorized as a very-high risk zone. The high population density, household density, LST and NDBI values, and the presence of built-up areas are the main reasons for the spread of dengue in the Thiruvananthapuram corporation. Neyyattinkara, Nedumangad, Attingal, and Varkala municipalities, and Navaikulam, Mudakkal, Mangalapuram, Kadinamkulam, Manikkal, Vembayam, Karakulam, Parassala, Aruvikkara, Vilappil, Poovachal, Kattakkada, Malayinkeezhu, Maranalloor, Pallichal, Balaramapuram, and Kalliyoor panchayats are categorized as high-risk zones. The Thiruvananthapuram corporation alone reported 3671 cases, and the other municipalities and panchayats categorized as high-risk zones together accounted for 2678 dengue cases. Around 82.87% of the dengue cases occurred in the very high and high-risk zones (Fig. 10).

This study found household density, population density, LST, NDBI, and LULC to be the most influential factors. The study by Ali and Ahmad (2018)

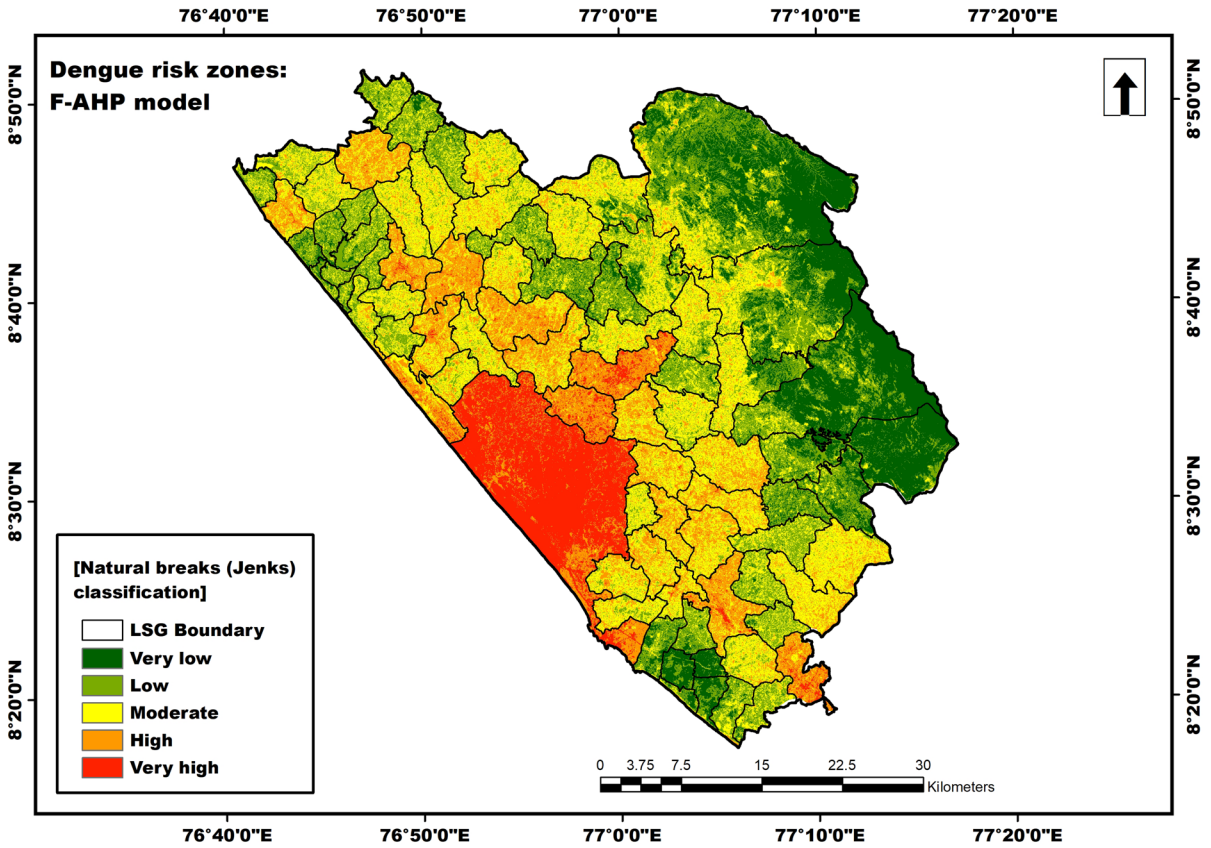

Fig. 8 Dengue risk zones: F-AHP model

Table 8 Percentage of risk zones

Risk zones	AHP method	F-AHP method
	Percentage of the area of risk zones	Percentage of the area of risk zones
Very low	16.04	16.53
Low	25.94	25.48
Moderate	30.18	30.60
High	18.71	18.30
Very high	9.13	9.09
Total	100	100

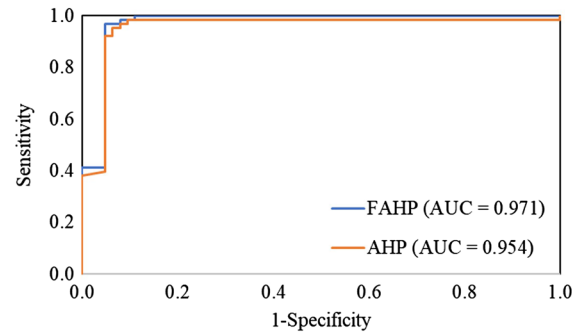

Fig. 9 The ROC curves

also found household density, population density, LST, and LULC as the most influential factors for dengue spread in Kolkata municipal corporation. They also listed elevation and waterlogged areas as influential factors. Withanage et al., (2021) found close proximity to roads and vegetation to be the most influential factors for high dengue risk in the Gampaha district, Sri Lanka. Tsheten et al., (2021) identified population density, LULC, and road connectivity as the three highly influential factors. However, road networks, water bodies/waterlogged areas, and climatic factors like rainfall have not been

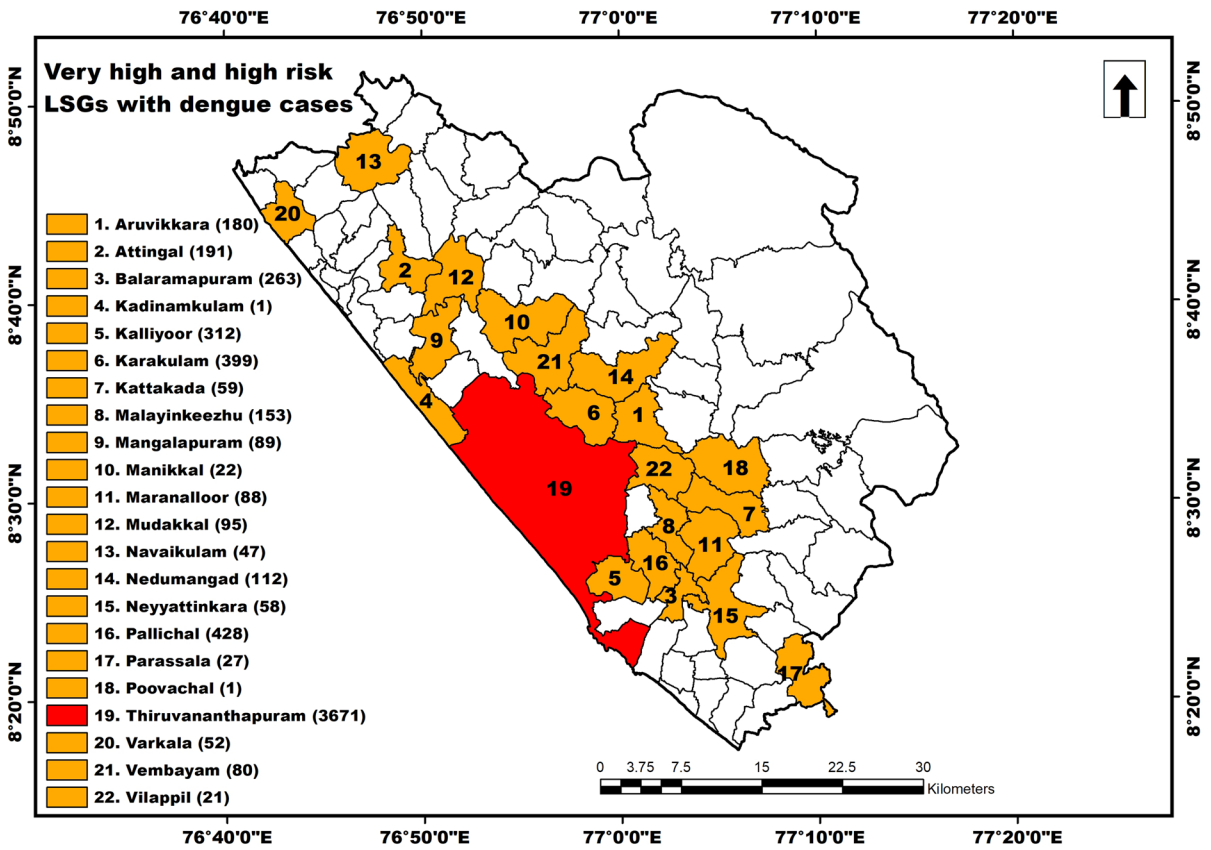

Fig. 10 Very high and high risk LSGs with dengue cases

included in this model. This is because, to assess the influence of developments, NDBI has been integrated. Similarly, instead of water bodies or waterlogged areas, factors like TWI have been included in the modelling. Because of the lack of precise rainfall data due to a lack of adequate rain gauges or automated weather stations, as well as the poor spatial resolution of the global dataset (http://www.worldclim.com/version2) and the India Meteorological Department's gridded data (https://www.imdpune.gov.in/Clim_Pred_LRF_New/Gridd_Data_Download.html), rainfall was not chosen as a factor in this study. In a study conducted in Kerala by Karunakaran et al., (2014), altered sensorium, hypertension, and patients over the age of 40 (who were 9.3 times more likely to die) were revealed to be independent predictors of dengue death. This underlines the need for vulnerability modelling by integrating socio-economic and physico-environmental indicators (as in Senan et al., 2022).

F-AHP can be employed to address AHP's incapacity to deal with subjectivity and irrationality in the decision maker's judgments (Carnero, 2017). This fact is confirmed by the prediction accuracy score (AUC value) of the maps created in this study. The studies by Akshaya et al., (2021), Meshram et al., (2019), Tripathi et al., (2021), and Senan et al., (2022) also found F-AHP as more effective than the AHP model. Validation of the created maps is the integral part of any modelling (susceptibility, risk, or vulnerability) due to the fact that "unless validated, the map is of no operational use". The ROC curve is one of the best techniques for validation (accuracy assessment) of maps. The creation of the ROC curve is challenging for this type of modelling, as the coordinates of houses with dengue cases are not available with the IDSP portal (https://dhs.kerala.gov.in/idsp-2/) of DHS. Therefore, in this study, one location from each LSG with dengue cases has been selected as a representation of the whole LSG for the validation. The study by Tsheten et al., (2021)

also validated their results using a similar approach, and this type of ROC validation can have a certain level of uncertainty. The dengue risk modelling by Ali and Ahmad (2018) also hasn't validated their results. In their study, Hassan et al., (2012), instead of validation by methods like ROC, compared the risk map with a map of actual dengue cases to assess the accuracy. The comparison of the risk map with the actual case data has been done in this study and also in the work by Ong et al., (2018) to assess the accuracy.

Conclusion

In this study, the risk zones for dengue in the Thiruvananthapuram district of Kerala were identified using the AHP and the F-AHP models. The dengue risk modelling utilized factors such as NDVI, LST, TWI, LULC, elevation, NDBI, household density, and population density. This study found that the F-AHP model (with an AUC of 97.1%) is more effective than the AHP model (with an AUC of 95.4%, or 0.954). Based on the F-AHP model, around 9.09% of the Thiruvananthapuram district is classified as a high-risk zone. This study identified Thiruvananthapuram corporation as a very high-risk zone, and four municipalities and 17 panchayats as high-risk zones. This study used the census data published in the year 2011, the only authentic data published by the government of India every 10 years. The latest population and household data are not available, as the 2021 census was not completed by the government due to the COVID-19 outbreak. Also, only the LSG-wise number of dengue cases is available on the DHS IDSP portal. If the geotagged dengue cases and precise rainfall data were integrated, the output could be greatly improved. These are the limitations of this study. The importance of this modelling is that the dengue hotspots can be predicted using these types of geo-environmental and demographic factors, and this will aid decision-makers, health professionals, and the government in identifying households located in high and very-high risk areas. It will help to strategize dengue-related projects in the future. This type of modelling can also be adopted for identifying hotspots for other types of water or vector-borne diseases, and this model can also be used as a base model for developing dengue risk models in other areas of similar geo-environmental conditions. By revising the input factors, this model can be applied to other areas with different geo-environmental settings. The risk zone map that has been created will be greatly beneficial in the development of appropriate preventive strategies for agencies/departments that deal with epidemics.

Acknowledgements The first author is thankful to the Directorate of Collegiate Education, Government of Kerala for funding this project with Aspire Scholarship (ASPR) 2020-21 (Reg. No. 010033197214). The authors would like to express their gratitude to the anonymous reviewers for their insightful comments on earlier versions of the manuscript.

Funding This study was funded by Directorate of Collegiate Education, Government of Kerala with Aspire Scholarship (ASPR) 2020–21 (Reg. No. 010033197214).

Availability of data and materials The datasets generated during and/or analyzed during the current study are available from the corresponding author on reasonable request.

Declarations

Conflicts of interest Disclosure of potential conflicts of interest The authors have no conflicts of interest to declare.

Ethical Approval This article does not contain any studies with human participants or animals performed by any of the authors.

Informed Consent Not applicable.

References

Afolayan, A. H., Ojokoh, B. A., & Adetunmbi, A. O. (2020). Performance analysis of fuzzy analytic hierarchy process multi-criteria decision support models for contractor selection. *Scientific African*. https://doi.org/10.1016/j.sciaf.2020.e00471

Akshaya, M., Danumah, J. H., Saha, S., Ajin, R. S., & Kuriakose, S. L. (2021). Landslide susceptibility zonation of the Western Ghats region in Thiruvananthapuram district (Kerala) using geospatial tools: A comparison of the AHP and Fuzzy-AHP methods. *Safety in Extreme Environments, 3*, 181–202. https://doi.org/10.1007/s42797-021-00042-0

Alam, A., Bhat, M. S., & Maheen, M. (2020). Using Landsat satellite data for assessing the land use and land cover change in Kashmir valley. *GeoJournal, 85*, 1529–1543. https://doi.org/10.1007/s10708-019-10037-x

Ali, S. A., & Ahmad, A. (2018). Using analytic hierarchy process with GIS for Dengue risk mapping in Kolkata Municipal Corporation, West Bengal, India. *Spatial Information Research, 26*, 449–469. https://doi.org/10.1007/s41324-018-0187-x

Amrutha, K., Danumah, J. H., Nikhil, S., Saha, S., Rajaneesh, A., Mammen, P. C., Ajin, R. S., & Kuriakose, S. L. (2022). Demarcation of forest fire risk zones in Silent Valley National Park and the effectiveness of forest management regime. *Journal of Geovisualization and Spatial Analysis*. https://doi.org/10.1007/s41651-022-00103-3

Arabameri, A., Saha, S., Roy, J., Chen, W., Blaschke, T., & Bui, D. T. (2020). Landslide susceptibility evaluation and management using different machine learning methods in the Gallicash river watershed, Iran. *Remote Sensing*. https://doi.org/10.3390/rs12030475

Artis, D. A., & Carnahan, W. H. (1982). Survey of emissivity variability in thermography of urban areas. *Remote Sensing of Environment, 12*(4), 313–329. https://doi.org/10.1016/0034-4257(82)90043-8

Ayhan, M. B. (2013). A fuzzy AHP approach for supplier selection problem: a case study in a gear motor company. *International Journal of Managing Value and Supply Chains, 4*(3), 11–23. https://doi.org/10.5121/ijmvsc.2013.4302

Babitha, B. G., Danumah, J. H., Pradeep, G. S., Costache, R., Patel, N., Prasad, M. K., Rajaneesh, A., Mammen, P. C., Ajin, R. S., & Kuriakose, S. L. (2022). A framework employing the AHP and FR methods to assess the landslide susceptibility of the Western Ghats region in Kollam district. *Safety in Extreme Environments, 4*, 171–191. https://doi.org/10.1007/s42797-022-00061-5

Balaji, D., & Saravanabavan, V. (2020). A geo medical analysis of dengue cases in Madurai city-Tamilnadu India. *GeoJournal, 85*, 979–994. https://doi.org/10.1007/s10708-019-10006-4

Banerjee, I. (2017). Dengue: The break-bone fever outbreak in Kerala. *India. Nepal Journal of Epidemiology, 7*(2), 666–669.

Battolla, E., Canessa, P. A., Ferro, P., Franceschini, M. C., Fontana, V., Dessanti, P., Pinelli, V., Morabito, A., Fedeli, F., Pistillo, M. P., & Roncella, S. (2017). Comparison of the diagnostic performance of fibulin-3 and mesothelin in patients with pleural effusions from malignant mesothelioma. *Anticancer Research, 37*(3), 1387–1391. https://doi.org/10.21873/anticanres.11460

Beven, K. J., & Kirkby, M. J. (1979). A physically based, variable contributing area model of basin hydrology. *Hydrological Sciences Journal, 24*(1), 43–69. https://doi.org/10.1080/02626667909491834

Bhatt, P., Sabeena, S. P., Varma, M., & Arunkumar, G. (2021). Current understanding of the pathogenesis of dengue virus infection. *Current Microbiology, 78*, 17–32. https://doi.org/10.1007/s00284-020-02284-w

Bhatt, S., Gething, P. W., Brady, O. J., Messina, J. P., Farlow, A. W., Moyes, C. L., Drake, J. M., Brownstein, J. S., Hoen, A. G., Sankoh, O., Myers, M. F., George, D. B., Jaenisch, T., Wint, G. R. W., Simmons, C. P., Scott, T. W., Farrar, J. J., & Hay, S. I. (2013). The global distribution and burden of dengue. *Nature, 496*, 504–507. https://doi.org/10.1038/nature12060

Buckley, J. J. (1985). Fuzzy Hierarchical Analysis. *Fuzzy Sets Systems, 17*(1), 233–247.

Carnero MC (2017) Benchmarking of the maintenance service in health care organizations. In: Noughabi E, Raahemi B, Albadvi A, Far B (eds) Handbook of research on data science for effective healthcare practice and administration. IGI Global, Hershey, Pennsylvania, United States, pp 1–25. http://doi:https://doi.org/10.4018/978-1-5225-2515-8.ch001

Chaturvedi, U., Agarwal, R., Elbishbishi, E., & Mustafa, A. (2000). Cytokine cascade in dengue hemorrhagic fever: Implications for pathogenesis. *FEMS Immunology & Medical Microbiology, 28*, 183–188. https://doi.org/10.1111/j.1574-695X.2000.tb01474.x

Chou, S. W., & Chang, Y. C. (2008). The implementation factors that influence the ERP (Enterprise Resource Planning) benefits. *Decision Support Systems, 46*(1), 149–157.

Choubin, B., Soleimani, F., Pirnia, A., Sajedi-Hosseini, F., Alilou, H., Rahmati, O., Melesse, A. M., Singh, V. P., & Shahabi, H. (2019). Chapter 17 - Effects of drought on vegetative cover changes: Investigating spatiotemporal patterns. In A. M. Melesse, W. Abtew, & G. Senay (Eds.), *Extreme hydrology and climate variability* (pp. 213–222). Amsterdam, Netherlands: Elsevier. https://doi.org/10.1016/B978-0-12-815998-9.00017-8

Cohen, J. M., Ernst, K. C., Lindblade, K. A., Vulule, J. M., John, C. C., & Wilson, M. L. (2010). Local topographic wetness indices predict household malaria risk better than land-use and land-cover in the western Kenya highlands. *Malaria Journal*. https://doi.org/10.1186/1475-2875-9-328

Dang, T., Yue, P., Bachofer, F., Wang, M., & Zhang, M. (2020). Monitoring land surface temperature change with landsat images during dry seasons in Bac Binh, Vietnam. *Remote Sensing*. https://doi.org/10.3390/rs12244067

Danumah, J. H., Odai, S. N., Saley, B. M., Szarzynski, J., Thiel, M., Kwaku, A., Kouame, F. K., & Akpa, L. Y. (2016). Flood risk assessment and mapping in Abidjan district using multi-criteria analysis (AHP) model and geoinformation techniques, (cote d'ivoire). *Geoenvironmental Disasters*. https://doi.org/10.1186/s40677-016-0044-y

DCHB (District Census Handbook). (2014). District census handbook – Thiruvananthapuram, Village and Town wise primary census abstract (PCA), Series-33, Part XII-B. Directorate of Census Operations, Kerala. Available at https://censusindia.gov.in/nada/index.php/catalog/665.

Dissanayake, D. S., Wijekoon, C. D., & Wegiriya, H. C. (2021). The effect of breeding habitat characteristics on the larval abundance of Aedes vector mosquitoes (Diptera: Culicidae) in three localities, Galle District, Sri Lanka. *Psyche: A Journal of Entomology*. https://doi.org/10.1155/2021/9911571

Dom, N. C., Ahmad, A. H., Latif, Z. A., & Ismail, R. (2016). Application of geographical information system-based analytical hierarchy process as a tool for dengue risk assessment. *Asian Pacific Journal of Tropical Disease, 6*(12), 928–935. https://doi.org/10.1016/S2222-1808(16)61158-1

Dom, N. C., Ahmad, A. H., Latif, Z. A., Ismail, R., & Pradhan, R. (2013). Coupling of remote sensing data and environmental-related parameters for dengue transmission risk assessment in Subang Jaya. *Malaysia. Geocarto*

International, 28(3), 258–272. https://doi.org/10.1080/10106049.2012.696726

Drisya, J., Sathish Kumar, D., & Roshni, T. (2018). Chapter 27 - Spatiotemporal variability of soil moisture and drought estimation using a distributed hydrological model. In P. Samui, D. Kim, & C. Ghosh (Eds.), *Integrating disaster science and management* (pp. 451–460). Amsterdam, Netherlands: Elsevier. https://doi.org/10.1016/B978-0-12-812056-9.00027-0

Eskandari, S., & Miesel, J. R. (2017). Comparison of the fuzzy AHP method, the spatial correlation method, and the Dong model to predict the fire high-risk areas in Hyrcanian forests of Iran. *Geomatics, Natural Hazards and Risk, 8*(2), 933–949. https://doi.org/10.1080/19475705.2017.1289249

Fan, J., Wei, W., Bai, Z., Fan, C., Li, S., Liu, Q., & Yang, K. (2015). A systematic review and meta-analysis of Dengue risk with temperature change. *International Journal of Environmental Research and Public Health, 12*(1), 1–15. https://doi.org/10.3390/ijerph120100001

Gessesse, A. A., & Melesse, A. M. (2019). Chapter 8 - Temporal relationships between time series CHIRPS-rainfall estimation and eMODIS-NDVI satellite images in Amhara Region, Ethiopia. In A. M. Melesse, W. Abtew, & G. Senay (Eds.), *Extreme hydrology and climate variability* (pp. 81–92). Amsterdam, Netherlands: Elsevier. https://doi.org/10.1016/B978-0-12-815998-9.00008-7

Getachew, D., Tekie, H., Gebre-Michael, T., Balkew, M., & Mesfin, A. (2015). Breeding sites of Aedes aegypti: potential dengue vectors in Dire Dawa, East Ethiopia. *Interdisciplinary Perspectives on Infectious Diseases*. https://doi.org/10.1155/2015/706276

Ghosh, S., Das, A., Hembram, T. K., Saha, S., Pradhan, B., & Alamri, A. M. (2020). Impact of COVID-19 induced lockdown on environmental quality in four Indian megacities using Landsat 8 OLI and TIRS-derived data and Mamdani fuzzy logic modelling approach. *Sustainability*. https://doi.org/10.3390/su12135464

Gompf, K., Traverso, M., & Hetterich, J. (2021). Using analytical hierarchy process (AHP) to introduce weights to social life cycle assessment of mobility services. *Sustainability*. https://doi.org/10.3390/su13031258

Govil, H., Guha, S., Dey, A., & Gill, N. (2019). Seasonal evaluation of downscaled land surface temperature: A case study in a humid tropical city. *Heliyon*. https://doi.org/10.1016/j.heliyon.2019.e01923

Hassan, H., Shohaimi, S., & Hashim, N. R. (2012). Risk mapping of dengue in Selangor and Kuala Lumpur. *Malaysia. Geospatial Health, 7*(1), 21–25. https://doi.org/10.4081/gh.2012.101

Hawley, W. A. (1988). The biology of Aedes albopictus. Journal of the American Mosquito Control Association. *Supplement, 1*, 1–39.

Honório, N. A., da Costa, S. W., Leite, P. J., Gonçalves, J. M., Lounibos, L. P., & Lourenço-de-Oliveira, R. (2003). Dispersal of Aedes aegypti and Aedes albopictus (Diptera: Culicidae) in an urban endemic dengue area in the State of Rio de Janeiro Brazil. *Memórias Do Instituto Oswaldo Cruz, 98*(2), 191–198. https://doi.org/10.1590/S0074-02762003000200005

Hoo, Z. H., Candlish, J., & Teare, D. (2017). What is an ROC curve? *Emergency Medicine Journal, 34*(6), 357–359. https://doi.org/10.1136/emermed-2017-206735

Karunakaran, A., Ilyas, W. M., Sheen, S. F., Jose, N. K., & Nujum, Z. T. (2014). Risk factors of mortality among dengue patients admitted to a tertiary care setting in Kerala, India. *Journal of Infection and Public Health, 7*(2), 114–120. https://doi.org/10.1016/j.jiph.2013.09.006

Khormi, H. M., & Kumar, L. (2012). Assessing the risk for dengue fever based on socioeconomic and environmental variables in a geographical information system environment. *Geospatial Health, 6*(2), 171–176. https://doi.org/10.4081/gh.2012.135

Kikuti, M., Cunha, G. M., Paploski, I. A. D., Kasper, A. M., Silva, M. M. O., Tavares, A. S., Cruz, J. S., Queiroz, T. L., Rodrigues, M. S., Santana, P. M., Lima, H. C. A. V., Calcagno, J., Takahashi, D., Gonçalves, A. H. O., Araújo, J. M. G., Gauthier, K., Diuk-Wasser, M. A., Kitron, U., Ko, A. I., … Ribeiro, G. S. (2015). Spatial distribution of dengue in a Brazilian urban slum setting: Role of socioeconomic gradient in disease risk. *PLoS Neglected Tropical Diseases*. https://doi.org/10.1371/journal.pntd.0003937

Koyadun, S., Butraporn, P., & Kittayapong, P. (2012). Ecologic and sociodemographic risk determinants for Dengue transmission in urban areas in Thailand. *Interdisciplinary Perspectives on Infectious Diseases*. https://doi.org/10.1155/2012/907494

Kumar, A., Agarwal, V., Pal, L., Chandniha, S. K., & Mishra, V. (2021a). Effect of land surface temperature on urban heat island in Varanasi City. *India. J, 4*(3), 420–429. https://doi.org/10.3390/j4030032

Kumar, N. P., Anish, T. S., Valamparampil, M. J., Thomas, A. T., Abidha, M. J., Ajithlal, P. M., & Jambulingam, P. (2019). Genotype shift of dengue virus (DENV1) during the 2017 outbreak of dengue fever in Thiruvananthapuram, Kerala, India. *Indian Journal of Experimental Biology, 57*, 961–966.

Kumar, N. P., Jayakumar, P. R., George, K., Kamaraj, T., Krishnamoorthy, K., Sabesan, S., & Jambulingam, P. (2013). Genetic characterization of dengue viruses prevalent in Kerala State India. *Journal of Medical Microbiology, 62*(4), 545–552. https://doi.org/10.1099/jmm.0.052696-0

Kumar, R., Dwivedi, S. B., & Gaur, S. (2021b). A comparative study of machine learning and Fuzzy-AHP technique to groundwater potential mapping in the data-scarce region. *Computers & Geosciences*. https://doi.org/10.1016/j.cageo.2021.104855

Lai, Y. H. (2018). The climatic factors affecting dengue fever outbreaks in southern Taiwan: an application of symbolic data analysis. *BioMedical Engineering OnLine*. https://doi.org/10.1186/s12938-018-0575-4

Landsat 8 Data Users Handbook (2019) Version 5.0, Department of the Interior, U.S. Geological Survey. Available online: https://www.usgs.gov/media/files/landsat-8-data-users-handbook.

Langkulsen, U., Sakolnakhon, K. P. N., & James, N. (2020). Climate change and dengue risk in central region of Thailand. *International Journal of Environmental Health Research, 30*(3), 327–335. https://doi.org/10.1080/09603123.2019.1599100

Latif, Z. A., Mohamad, M. H., (2015). Mapping of dengue outbreak distribution using spatial statistics and geographical information system. In: *Proceedings of the 2nd international conference on information science and security (ICISS)*, pp. 1–6, https://doi.org/10.1109/ICISSEC.2015.7371016.

Lowe, R., Lee, S. A., O'Reilly, K. M., Brady, O. J., Bastos, L., Carrasco-Escobar, G., Catão, Rd. C., Colón-González, F. J., Barcellos, C., Carvalho, M. S., Blangiardo, M., Rue, H., & Gasparrini, A. (2021). Combined effects of hydrometeorological hazards and urbanisation on dengue risk in Brazil: A spatiotemporal modelling study. *The Lancet Planetary Health, 5*(4), e209–e219. https://doi.org/10.1016/S2542-5196(20)30292-8

Meshram, S. G., Alvandi, E., Singh, V. P., & Meshram, C. (2019). Comparison of AHP and fuzzy AHP models for prioritization of watersheds. *Soft Computing, 23*, 13615–13625. https://doi.org/10.1007/s00500-019-03900-z

Messina, J. P., Brady, O. J., Golding, N., Kraemer, M. U. G., Wint, G. R. W., Ray, S. E., Pigott, D. M., Shearer, F. M., Johnson, K., Earl, L., Marczak, L. B., Shirude, S., Weaver, N. D., Gilbert, M., Velayudhan, R., Jones, P., Jaenisch, T., Scott, T. W., Reiner, R. C., Jr., & Hay, S. I. (2019). The current and future global distribution and population at risk of dengue. *Nature Microbiology, 4*, 1508–1515. https://doi.org/10.1038/s41564-019-0476-8

Mustafa, M. S., Rasotgi, V., Jain, S., & Gupta, V. (2015). Discovery of fifth serotype of dengue virus (DENV-5): a new public health dilemma in dengue control. *Medical Journal Armed Forces India, 71*(1), 67–70. https://doi.org/10.1016/j.mjafi.2014.09.011

Nair, D. G., & Aravind, N. P. (2020). Association between rainfall and the prevalence of clinical cases of dengue in Thiruvananthapuram district, India. *International Journal of Mosquito Research, 7*(6), 46–50. https://doi.org/10.22271/23487941.2020.v7.i6a.488

Nakano, K. (2018). Future risk of dengue fever to workforce and industry through global supply chain. *Mitigation and Adaptation Strategies for Global Change, 23*, 433–449. https://doi.org/10.1007/s11027-017-9741-4

Ngugi, H. N., Mutuku, F. M., Ndenga, B. A., Musunzaji, P. S., Mbakaya, J. O., Aswani, P., Irungu, L. W., Mukoko, D., Vulule, J., Kitron, U., & LaBeaud, A. D. (2017). Characterization and productivity profiles of Aedes aegypti (L) breeding habitats across rural and urban landscapes in western and coastal Kenya. *Parasites Vectors*. https://doi.org/10.1186/s13071-017-2271-9

Nichol, J. E. (1994). A GIS-based approach to microclimate monitoring in Singapore's high-rise housing estates. *Photogrammetric Engineering and Remote Sensing, 60*, 1225–1232.

Nikhil, S., Danumah, J. H., Saha, S., Prasad, M. K., Rajaneesh, A., Mammen, P. C., Ajin, R. S., & Kuriakose, S. L. (2021). Application of GIS and AHP method in forest fire risk zone mapping: a study of the Parambikulam Tiger Reserve, Kerala, India. *Journal of Geovisualization and Spatial Analysis*. https://doi.org/10.1007/s41651-021-00082-x

Nujum, Z. T., Beegum, M. S., Meenakshy, V., & Vijayakumar, K. (2020). Cost analysis of dengue from a State in south India. *Indian Journal of Medical Research, 152*(5), 490–497. https://doi.org/10.4103/ijmr.IJMR_1641_18

Ong, J., Liu, X., Rajarethinam, J., Kok, S. Y., Liang, S., Tang, C. S., Cook, A. R., Ng, L. C., & Yap, G. (2018). Mapping dengue risk in Singapore using random forest. *PLoS Neglected Tropical Diseases*. https://doi.org/10.1371/journal.pntd.000658

Panhwer, M. A., Pirzada, N., Abro, A., & Khahro, S. H. (2017). Spatial risk mapping for dengue fever using GIS: a case study of Hyderabad. *Sindh University Research Journal (science Series), 49*(1), 93–96.

Pathirana, S., Kawabata, M., & Goonatilake, R. (2009). Study of potential risk of dengue disease outbreak in Sri Lanka using GIS and statistical modelling. *Journal of Rural and Tropical Public Health, 8*, 8–17.

Pilot, E., Murthy, G. V. S., & Nittas, V. (2020). Understanding India's urban dengue surveillance: A qualitative policy analysis of Hyderabad district. *Global Public Health, 15*(11), 1702–1717. https://doi.org/10.1080/17441692.2020.1767674

Pradeep, G. S., Danumah, J. H., Nikhil, S., Prasad, M. K., Patel, N., Mammen, P. C., Rajaneesh, A., Oniga, V. E., Ajin, R. S., & Kuriakose, S. L. (2022). Forest fire risk zone mapping of Eravikulam National Park in India: a comparison between frequency ratio and analytic hierarchy process methods. *Croatian Journal of Forest Engineering, 43*(1), 199–217. https://doi.org/10.5552/crojfe.2022.1137

Qazi, W. A. (2020). Abushammala MFM (2020) Chapter 10 - Multi-criteria decision analysis of waste-to-energy technologies. In J. Ren (Ed.), *waste-to-energy* (pp. 265–316). Cambridge: Academic Press. https://doi.org/10.1016/B978-0-12-816394-8.00010-0

Ramkar, P., & Yadav, S. M. (2021). Flood risk index in data-scarce river basins using the AHP and GIS approach. *Natural Hazards, 109*, 1119–1140. https://doi.org/10.1007/s11069-021-04871-x

Rani, V. R. (2013). Ground water information booklet of Trivandrum district, *Kerala state. Technical reports: Series D, central ground water board kerala region, Ministry of Water Resources*, Government of India.

Rasheed, S. B., Butlin, R. K., & Boots, M. (2013). A review of dengue as an emerging disease in Pakistan. *Public Health, 127*(1), 11–17. https://doi.org/10.1016/j.puhe.2012.09.006

Reis, S. (2008). Analyzing land use/land cover changes using remote sensing and GIS in Rize North-East Turkey. *Sensors, 8*(10), 6188–6202. https://doi.org/10.3390/s8106188

Riadi, B., Barus, B., Widiatmaka Yanuar, MJP., Pramudya, B. (2018). Identification and delineation of areas flood hazard using high accuracy of DEM data. In: *IOP Conference Series: Earth and Environmental Science, Vol. 149, The 4th International Symposium on LAPAN-IPB Satellite for Food Security and Environmental Monitoring,* 9-11 October 2017, Bogor, Indonesia. https://doi.org/10.1088/1755-1315/149/1/012035.

Rogers, D. J., Suk, J. E., & Semenza, J. C. (2014). Using global maps to predict the risk of dengue in Europe. *Acta Tropica, 129*, 1–14. https://doi.org/10.1016/j.actatropica.2013.08.008

Rouse, J. W., Haas, R. H., Schell, J. A., & Deering, D. W. (1974). Monitoring vegetation systems in the Great Plains with ERTS. In S. C. Freden, E. P. Mercanti, & M. A. Becker (Eds.), *Proceedings of the third earth resources technology satellite-1 symposium* (pp. 309–317). Washington DC, USA: NASA.

Saaty, T. L. (1980). *The analytic hierarchy process: planning, priority setting, resource allocation (Decision making series)*. New York: McGraw Hill.

Samuel, P. P., Thenmozhi, V., Nagaraj, J., Kumar, T. D., & Tyagi, B. K. (2014). Dengue vectors prevalence and the related risk factors involved in the transmission of dengue in Thiruvananthapuram district, Kerala, South India. *Journal of Vector Borne Diseases, 51*(4), 313–319.

Saravanabavan, V., Balaji, D., & Preethi, S. (2019). Identification of dengue risk zone: a geo-medical study on Madurai city. *GeoJournal, 84*, 1073–1087. https://doi.org/10.1007/s10708-018-9909-9

Saravanan, S., Jegankumar, R., Selvaraj, A., Jennifer, J. J., & Parthasarathy, K. S. S. (2019). Chapter 20 Utility of Landsat data for assessing mangrove degradation in Muthupet Lagoon South India. In M. Ramkumar, R. A. James, D. Menier, & K. Kumaraswamy (Eds.), *Coastal zone management* (pp. 471–484). Amsterdam, Netherlands: Elsevier. https://doi.org/10.1016/B978-0-12-814350-6.00020-3

Sarfraz, M. S., Tripathi, N. K., Tipdecho, T., Thongbu, T., Kerdthong, P., & Souris, M. (2012). Analyzing the spatio-temporal relationship between dengue vector larval density and land-use using factor analysis and spatial ring mapping. *BMC Public Health*. https://doi.org/10.1186/1471-2458-12-853

Schmidt, W. P., Suzuki, M., Dinh Thiem, V., White, R. G., Tsuzuki, A., Yoshida, L. M., Yanai, H., Haque, U., Tho, L. H., Anh, D. D., & Ariyoshi, K. (2011). Population density, water supply, and the risk of dengue fever in Vietnam: Cohort study and spatial analysis. *PLoS Medicine, 8*(8), e10001082. https://doi.org/10.1371/journal.pmed.1001082

Senan, C. P. C., Ajin, R. S., Danumah, J. H., Costache, R., Arabameri, A., Rajaneesh, A., Sajinkumar, K. S., & Kuriakose, S. L. (2022). Flood vulnerability of a few areas in the foothills of the Western Ghats: a comparison of AHP and F-AHP models. *Stochastic Environmental Research and Risk Assessment*. https://doi.org/10.1007/s00477-022-02267-2

Shabbir, W., Pilz, J., & Naeem, A. (2020). A spatial-temporal study for the spread of dengue depending on climate factors in Pakistan (2006–2017). *BMC Public Health*. https://doi.org/10.1186/s12889-020-08846-8

Shafie, A. (2011). Evaluation the spatial risk factors for high incidence of dengue fever and dengue hemorrhagic fever using GIS application. *Sains Malaysiana, 40*(8), 937–943.

Snyder, W. C., Wan, Z., Zhang, Y., & Feng, Y. Z. (1998). Classification-based emissivity for land surface temperature measurement from space. *International Journal of Remote Sensing, 19*(14), 2753–2774. https://doi.org/10.1080/014311698214497

Tabachnick, W., Munstermann, L., & Powell, J. (1979). Genetic distinctness of sympatric forms of Aedes aegypti in East Africa. *Evolution, 33*(1), 287–295. https://doi.org/10.2307/2407619

Tariq, B., & Zaidi, A. Z. (2019). Geostatistical modeling of dengue disease in Lahore Pakistan. *SN Applied Sciences*. https://doi.org/10.1007/s42452-019-0428-1

Telle, O., Nikolay, B., Kumar, V., Benkimoun, S., Pal, R., Nagpal, B., & Paul, R. E. (2021). Social and environmental risk factors for dengue in Delhi city: A retrospective study. *PLoS Neglected Tropical Diseases, 15*(2), e0009024. https://doi.org/10.1371/journal.pntd.0009024

Thomas, A. V., Saha, S., Danumah, J. H., Raveendran, S., Prasad, M. K., Ajin, R. S., & Kuriakose, S. L. (2021). Landslide susceptibility zonation of Idukki district using GIS in the aftermath of 2018 Kerala floods and landslides: a comparison of AHP and frequency ratio methods. *Journal of Geovisualization and Spatial Analysis, 5*(2), 1–27. https://doi.org/10.1007/s41651-021-00090-x

Tripathi, A. K., Agrawal, S., & Gupta, R. D. (2021). Comparison of GIS-based AHP and fuzzy AHP methods for hospital site selection: a case study for Prayagraj City, India. *GeoJournal*. https://doi.org/10.1007/s10708-021-10445-y

Tsheten, T., Clements, A. C. A., Gray, D. J., & Wangdi, K. (2021). Dengue risk assessment using multicriteria decision analysis: a case study of Bhutan. *PLoS Neglected Tropical Diseases, 15*(2), e0009021. https://doi.org/10.1371/journal.pntd.0009021

Valson, J. S., & Soman, B. (2017). Spatiotemporal clustering of dengue cases in Thiruvananthapuram district. *Kerala. Indian Journal of Public Health, 61*(2), 74–80.

Viana, C. M., Oliveira, S., Oliveira, S. C., & Rocha, J. (2019). Land use/land cover change detection and urban sprawl analysis. In H. R. Pourghasemi & C. Gokceoglu (Eds.), *Spatial modeling in GIS and R for earth and environmental sciences* (pp. 621–651). Amsterdam, Netherlands: Elsevier.

Vojteková, J., & Vojtek, M. (2020). Assessment of landslide susceptibility at a local spatial scale applying the multicriteria analysis and GIS: A case study from Slovakia. *Geomatics, Natural Hazards and Risk, 11*(1), 131–148. https://doi.org/10.1080/19475705.2020.1713233

Wijayanti, S. P. M., Porphyre, T., Chase-Topping, M., Rainey, S. M., McFarlane, M., Schnettler, E., Biek, R., & Kohl, A. (2016). The importance of socio-economic versus environmental risk factors for reported dengue cases in Java. *Indonesia. Plos Neglected Tropical Diseases, 10*(9), e0004964. https://doi.org/10.1371/journal.pntd.0004964

Withanage, G. P., Gunawardana, M., Viswakula, S. D., Samaraweera, K., Gunawardena, N. S., & Hapugoda, M. D. (2021). Multivariate spatio-temporal approach to identify vulnerable localities in dengue risk areas using geographic information system (GIS). *Scientific Reports*. https://doi.org/10.1038/s41598-021-83204-1

Zeng, Z., Zhan, J., Chenc, L., Chen, H., & Cheng, S. (2021). Global, regional, and national dengue burden from 1990 to 2017: A systematic analysis based on the global burden of disease study 2017. *EclinicalMedicine*. https://doi.org/10.1016/j.eclinm.2020.100712

Zha, Y., Gao, J., & Ni, S. (2003). Use of normalized difference built-up index in automatically mapping urban areas from

TM imagery. *International Journal of Remote Sensing, 24*(3), 583–594. https://doi.org/10.1080/01431160304987